JOURNAL OF CATALYSIS **148**, 68–75 (1994)

Vapour-Phase Substitution of Chlorobenzene with Ammonia, Catalyzed by Copper-Exchanged Zeolites

M. H. W. Burgers and H. van Bekkum[1]

Laboratory of Organic Chemistry and Catalysis, Delft University of Technology, Julianalaan 136, 2628 BL Delft, The Netherlands

Received May 24, 1993; revised January 4, 1994

The nucleophilic substitution of chlorobenzene with ammonia, leading to aniline, was investigated over various copper-exchanged catalysts using vapour-phase reactants. Benzene and diphenylamine were formed as side-products. The zeolites tested (Cu–L, Cu–mordenite, Cu–Y, Cu–ZSM-5, and Cu–beta) gave better results than copper-containing silica–alumina, because of the high deactivation rate of the latter. On zeolites Cu–L, Cu–mordenite, and Cu–ZSM-5, substitution prevailed: with Cu–mordenite and Cu–ZSM-5, aniline selectivities of 90–94% were obtained. In contrast, reduction towards benzene was pronounced on Cu–beta and especially on Cu–Y. In more detailed studies with Cu–mordenite, two deactivation regimes were observed, related to the reaction temperature. With Cu–L, the dehalogenation towards benzene was investigated: it is ascribed to copper reduction, followed by the reduction of chlorobenzene with the copper(0) particles thus obtained.

INTRODUCTION

Nucleophilic substitution of organic halides is a type of reaction frequently encountered in aliphatic as well as in aromatic chemistry. In the latter case, dissolved copper salts are often used as homogeneous catalysts. The order of reactivity of the halogenated aromatics is generally I > Br > Cl ≫ F. At lower temperatures only relatively reactive substrates (organic halide reactants) can be converted, e.g., the substitution of bromobenzene with sodium methoxide at 80°C (1). Chlorobenzene derivatives, which are the most interesting starting materials from an economic point of view, are relatively inert. Either activating substituents, such as *ortho* nitro, must be present, or higher reaction temperatures must be applied (2).

The nucleophilic substitution of chlorobenzene (denoted as PhCl) with ammonia, shown in Fig. 1, is an example of a reaction in which nonactivated starting materials are used. To accomplish large-scale applications, it is important to investigate the possibilities of heterogeneous catalysis; in particular, zeolite catalysts may lead to interesting results, as the spatial constraints of the channel system can result in selectivity improvements (3). Using vapour-phase reactants, this amination has been studied before with zeolite-based catalysts. For copper-exchanged zeolite X, a conversion of 16–20% was reported at 370°C, with an amine selectivity of 52–55% and benzene as a side-product (4, 5); in another study, samples of metal-exchanged zeolite Y were compared using pulse experiments. The activity of the different metals decreased as follows: Cu > Ni > Zn, Cr > Co > Cd > Mn > Mg, Ca, Na ≈ 0. Using copper-exchanged Y (abbreviated as Cu–Y), a conversion of 38.7% was observed at 395°C with an aniline selectivity of 75% (6). Again, benzene was reported to be the main side-product. In all these reports, benzene selectivity was found to increase at higher temperatures.

Nonactivated nucleophilic substitutions using different starting materials have been investigated more recently. Phenol and anisole were converted with ammonia to aniline at temperatures exceeding 400°C on both proton-exchanged and copper-exchanged zeolite Y (7, 8); a better catalyst stability was obtained with H–ZSM-5 (8, 9). The latter catalyst was also reported to convert chlorobenzene with methanol to anisole (10); however, the selectivity was limited, side-reactions being methylation, dechlorination, and presumably methanol oligomerization. In the phenol/ammonia reaction, some other side-reactions were observed: the aniline formed was converted into diphenylamine on both Cu–Y (11) and H–ZSM-5 (12), and aniline was also rearranged at 510°C into 2-methylpyridine on H–ZSM-5 (12). However, the latter reaction, proceeding via a Michael-type ammonia addition (13), required increased pressures (e.g., 28 bar) to take place.

The formation of phenol from chlorobenzene and water has also been investigated using copper-exchanged zeolites: several materials with the MFI-structure were used (14, 15), leading to conversions of 35 to 45% at 450°C, with high selectivity (14). Use of nickel-exchanged ZSM-5 was reported to give a slightly higher phenol yield (16).

---

[1] Fax: (+31-15)782655.

0021-9517/94 $6.00

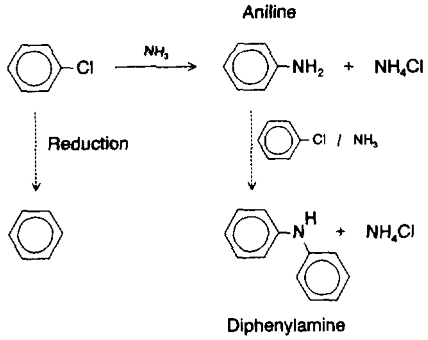

FIG. 1. Reaction scheme of the nucleophilic substitution of chlorobenzene with ammonia to aniline, with benzene and diphenylamine as side-products.

Copper-exchanged zeolites have received increasing attention recently, as they have proved to be active catalysts for NO_x decomposition (17), NO_x reduction with NH_3 (18) or with hydrocarbons (19), ammoxidation of toluene to benzonitrile (20, 21), and Diels–Alder dimerization of butadiene (22, 23). The latter reaction was catalyzed by copper-exchanged zeolite Y; it was mentioned that Cu^+ was the catalytic active site, and when Cu(II)–Y was used, the catalyst was first reduced to the Cu(I)/H–Y form. This reduction was performed by ammonia or by butadiene; a second order in the Cu^{2+} concentration was found, and the reduction was enhanced by a lower activation temperature, which was ascribed to the presence of residual water (24).

In the present paper, we report on the properties of copper-exchanged zeolites in the vapour-phase chlorobenzene substitution with ammonia. Four large-pore zeolites (Y, beta, L, and mordenite) and the medium-pore zeolite ZSM-5 have been compared; as the formation of benzene as a side-product seems to be important in the process, we have investigated its formation mechanism.

EXPERIMENTAL

Zeolite K–L was synthesized according to Wortel (25), example 1; Na–beta was synthesized according to Wadlinger *et al.* (26), example 7. Silica–alumina (LA-SHPV) and zeolite Na–Y were obtained from Akzo Chemical Division, mordenite from Union Carbide, and Na–ZSM-5 from VAW Aluminium Bonn.

Silica-alumina was treated three times with 1 *M* aqueous sodium nitrate for 8 h at 75°C, and exchanged once with 80 m*M* copper(II)nitrate under the same conditions. Cu/Na–ZSM-5 was prepared by ion exchange with 0.1 *M* copper(II)acetate overnight at room temperature; Cu/Na–Y by a single exchange with 10 m*M* copper(II)nitrate for 8 h at 75°C. Other copper-containing materials (denoted as Cu/*Me*-zeolite, where *Me* is the partially replaced counterion) were prepared by triple ion-exchange with a 20 m*M* (Cu–beta, Cu/Na-mordenite and Cu/K–L-2.8, a sample having 2.8 wt% copper) or an 80 m*M* (Cu/K–L-3.4) copper(II)nitrate solution for 8 h at 75°C.

For comparison, a physical mixture of 0.37 g copper(I) oxide and 3.6 g as-synthesized K–L, denoted as Cu_2O/K–L, was prepared by grinding, followed by heating to 475°C in a flow of nitrogen. A sample denoted as ($CuCl_2$)K–L was prepared by impregnation of as-synthesized K–L with copper(II)chloride, followed by water evaporation at 80°C. XRD analysis of this sample showed no $CuCl_2$ peaks.

The chemical compositions of all catalysts used for screening, as determined by Atomic Absorption or Emission Spectrometry, are given in Table 1.

Ammonia-TPD was performed by heating 100 mg samples to 500°C, followed by a reduction of Cu^{2+} to Cu^+ by ammonia at 400°C for the copper-containing samples; after cooling, ammonia was adsorbed at 100°C. During the actual measurement, the temperature was raised at 5°C/min, while nitrogen at a flow rate of 10 ml/min was used as carrier gas. Detection was performed by TCD.

Thermogravimetric analysis was performed by heating 65 to 85 mg used catalyst at 5°C/min up to 450°C in nitrogen (2.6 l/h); after cooling to room temperature, the measurement was performed by a thermal treatment with an identical temperature program in air (2.6 l/h).

For catalytic tests the catalysts were pelletized, crushed, and sieved; the fraction with a diameter between 0.7 and 1.0 mm was collected. One gram of material, stored under ambient, was used for each run. Reactions were performed at atmospheric pressure, downflow, in a borosilicate glass tube (i.d. 7 mm) heated by a fluidized bed oven.

TABLE 1

Chemical Compositions of the Catalysts Screened (the Absolute Copper Content Is Given for a Zeolite in the Hydrated State)

Sample name	Catalyst composition (normalised on aluminium)					Copper content (wt%)[a]
	Si	Al	Cu	K	Na	
Cu/K–L-2.8	2.7	1	0.14	n.d.	0	2.8
Cu/K–L-3.4	2.8	1	0.18	0.62	0	3.4
NH_4/K–L	2.7	1	0	0.50	0	0
($CuCl_2$)K–L	2.6	1	0.16	1	0	3.1
Cu/Na–Y	2.5	1	0.15	0	0.7	3.2
Cu-beta	14	1	0.43	n.d.	n.d.	2.4
Cu/Na–mordenite	10.2	1	0.32	n.d.	0.3	2.5
Cu/Na–ZSM-5	13.5	1	0.33	0	0.39	2.8
Cu_2O/K–L[b]	Cu_2O 9 wt%/K–L 91 wt%					8
Cu–silica–alumina	Al_2O_3 12 wt%					1.2

Note. n.d., not determined.
[a] Error in absolute copper amount, about ±10%.
[b] Physical mixture.

Before the amination experiments, copper(II)-based materials were pretreated: the reduction of copper(II) to copper(I) was accomplished with ammonia (2.4 ml/min) in presence of water (3.8 kPa in an N_2 stream of 45 ml/min) at 400°C (24), while the reduction to $Cu^0/2H^+$, to investigate the catalytic properties of metallic copper-based materials, was performed at 400°C in an H_2/N_2 stream (both 20 ml/min) containing 3.8 kPa water. The latter reduction was performed in the presence of water because its presence is reported to lead to small copper clusters (27); the presence of these clusters was observed with XRD.

During reactions, the feed gas consisted of predried nitrogen containing 16.5 vol% ammonia and 0.84 vol% chlorobenzene (molar ratio 20). The total flow rate was 33.4 ml/min; the WHSV (20°C) was $2.26\ h^{-1} \cdot (g_{total\ gas}/g_{cat})$. The ammonium chloride, produced as a side-product, was removed by a rapid temperature drop of the product gas to 250°C. Analysis was performed by on-line GC, product identification by GC-MS.

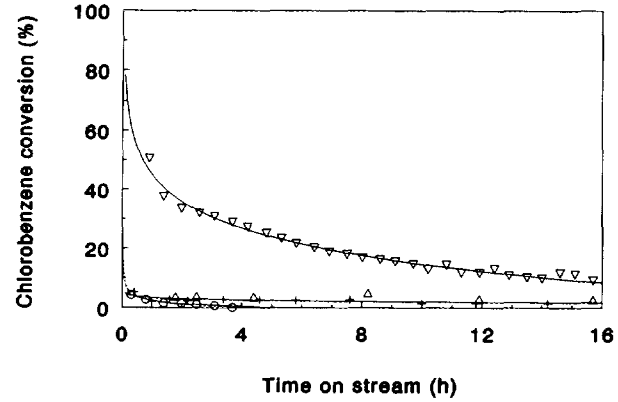

FIG. 3. Chlorobenzene conversion vs time on stream in the reaction with ammonia, using different catalysts: copper-exchanged silica-alumina (+), a physical mixture Cu_2O with K–L (○), NH_4/K–L (△), and Cu/K–L-2.8 (▽). Reaction temperature, 400°C.

RESULTS

1. Characterization by NH_3-Temperature Programmed Desorption

The as-synthesized Cu(II)–zeolites were reduced with ammonia (in a pretreatment or by the ammonia in the reaction feed) to the $Cu(I)/NH_4^+$ form (24, 28). To investigate the acidity thus obtained, characterization with NH_3 TPD was performed; desorption data of four zeolite-L-based materials are given in Fig. 2. NH_4/K–L has a desorption peak at about 480°C, caused by the decomposition of NH_4^+. In Cu(I)/NH_4/K–L, formed upon the reduction of Cu(II)/K–L with NH_3, the acid activity is indicated by the fact that this sample also shows a desorption peak at about 480°C, just like NH_4/K–L. The peak at intermediate temperature, about 375°C, is ascribed to the (partial) decomposition of copper(I)–ammonia complexes. It is also observed in (CuCl)K–L, the reduced form of the ($CuCl_2$)K–L sample. The absence of acid activity in the latter material is shown by the absence of a distinct 480°C peak.

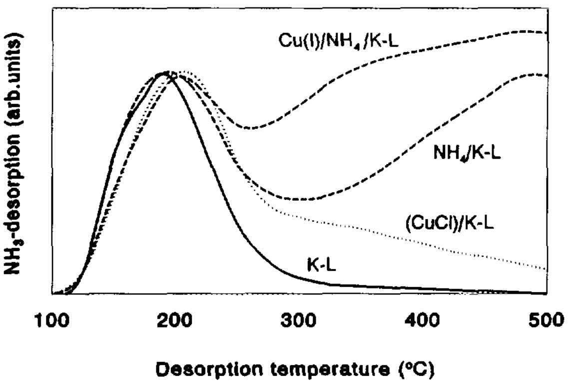

FIG. 2. TPD plots of as-synthesized K–L, NH_4/K–L, Cu(I)/NH_4/K–L-3.4, and (CuCl)/K–L. The latter two samples were obtained from Cu(II)/K–L and ($CuCl_2$)/K–L by NH_3-treatment at 400°C. Nitrogen flow rate, 10 ml/min; heating rate, 5°C/min.

2. Catalyst Screening

The catalytic performance of different copper-exchanged materials in the chlorobenzene amination, comparing a copper-exchanged zeolite with similar systems, is shown in Fig. 3. Aniline, diphenylamine and benzene were the main products. As-synthesized K–L and H/K–L (50% exchange) were essentially inactive (the conversion was within the limits of experimental error, max. 3%). Apparently copper is the actual catalytic active site under the conditions used. Moreover, the very low conversion obtained with the physical mixture Cu_2O/K–L shows that isolated copper-ions as present in copper-exchanged zeolites are needed to perform the catalytic process.

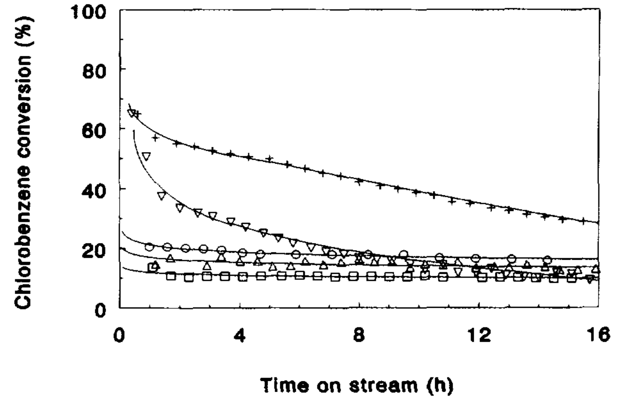

FIG. 4. Chlorobenzene conversion vs time on stream in the reaction with ammonia, using different catalysts: Cu/Na–Y (+), Cu-beta (△), Cu/K–L-2.8 (▽), Cu/Na–mordenite (○), and Cu/Na–ZSM-5 (□). Reaction temperature, 400°C.

TABLE 2

Selectivities of the Reactions Shown in Fig. 2[a]

Time on stream (h)	Cu-Y[b]		Cu-beta		Cu-L		Cu-mordenite		Cu-ZSM-5	
	$PhNH_2$ (%)	PhH (%)	$PhNH_2$ (%)	PhH (%)	$PhNH_2$ (%)	PhH (%)	$PhNH_2$ (%)	PhH (%)	$PhNH_2$ (%)	PhH (%)
1	40 ± 5	45 ± 5	54	25	54	2	90 ± 4	3	90	<2
3	6	77	48	35	60	1.9	93	3	91	<2
12	8	76	31	54	70	<0.5	94	3	92	<2
16	8	74	34	53	70	<0.5	—	—	—	—

[a] Besides the mentioned products, the balance is completed by formation of diphenylamine.

[b] Only with Cu-Y was another product formed, identified by GC-MS as 1,2-dichlorobenzene (selectivity 15–20%).

Cu-silica-alumina gave (based on the observation that ammonium chloride was formed) some initial activity, but had a very high deactivation rate. Already the first measurement after ½ h on stream showed a conversion as low as 5%, although there was negligible copper loss, <5% after 16 h on stream. This deactivation shows that the specific properties of the zeolites are important for maintaining stable catalyst activity.

In Fig. 4 and Table 2 various zeolites are compared. The data show that Cu-Y and Cu-L have a relatively high (initial) activity, and that the selectivity towards aniline is highly dependent on the type of zeolite used.

To investigate the influence of the acid activity caused by the reduction of Cu(II) to Cu(I) ions, a sample of $(CuCl_2)$K-L, an acid-free material (*vide infra*), was also tested for its amination activity. The results, shown in Fig. 5, indicate that this catalyst has a low but constant activity at 400°C.

Cu-mordenite was selected for kinetic investigations, because of its high aniline selectivity (>90%; see Table 2) and especially because of its low deactivation. The latter allows comparison of both initial conversions and conversions after prolonged time on stream. To examine the reaction order, the chlorobenzene vapour pressure was varied between 0.2 and 0.84 vol% at 400°C. The initial chlorobenzene conversion remained essentially equal, suggesting a first order reaction in chlorobenzene; a lower chlorobenzene vapour pressure did result in a slightly lower deactivation rate. To examine the influence of the reaction temperature, plots of $(\ln(1\text{-conversion})^{-1})$ vs the reciprocal temperature are shown in Fig. 6 for the initial reaction rate (extrapolated to $t = 0$) and the rate after prolonged (>16 h) time on stream. The data show that the initial rates exhibit a variation which resembles the straight line expected for a single first-order reaction. However, the rates after prolonged time on stream indicate that two regimes with different rate-limiting steps or different deactivation patterns exist above and below 400°C.

3. Catalyst Regeneration

In the experiments with large-pore zeolites Cu-Y and Cu-L, a high initial activity was found, along with a rapid catalyst deactivation. Therefore, these materials were very suitable for investigating catalyst regeneration. The

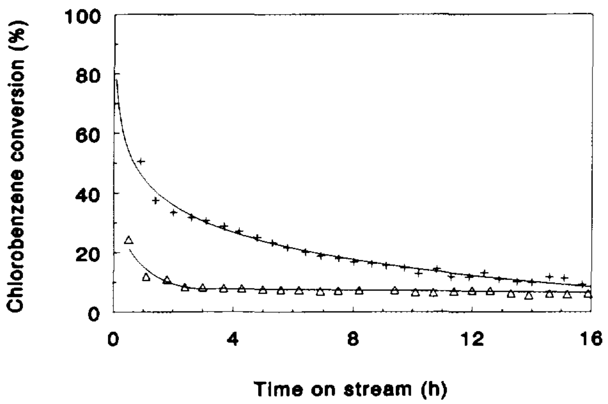

FIG. 5. Chlorobenzene conversion vs time on stream in the reaction with ammonia, catalyzed by Cu/K-L (+) and (CuCl)/K-L (△), the reduced form of $(CuCl_2)$K-L. Reaction temperature, 400°C.

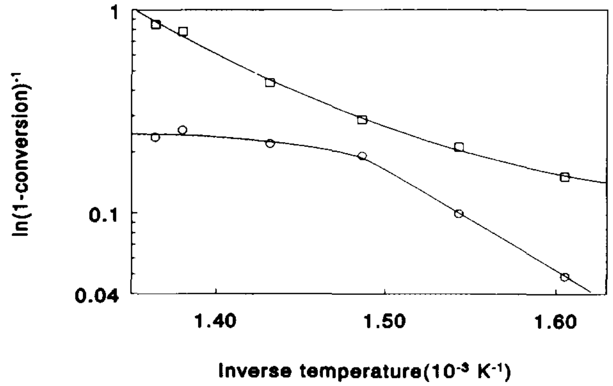

FIG. 6. Logarithmic plot of $\ln(1 - \text{chlorobenzene conversion})^{-1}$ vs reciprocal reaction temperature in the reaction with ammonia, catalyzed by Cu/Na-mordenite: initial conversions (□) and conversions after prolonged (>16 h) time on stream (○).

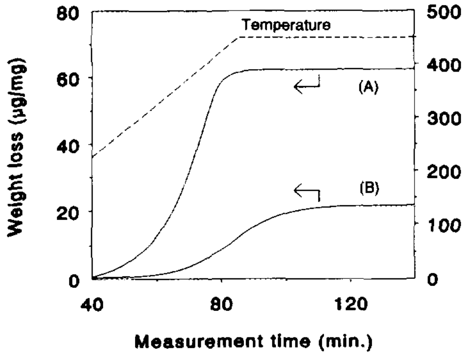

FIG. 7. TGA plot of Cu/K-L-3.4 (A) and Cu-silica-alumina (B), after use in a 16-h chlorobenzene amination experiment, heated in a stream of air. The material was activated in nitrogen prior to the measurement.

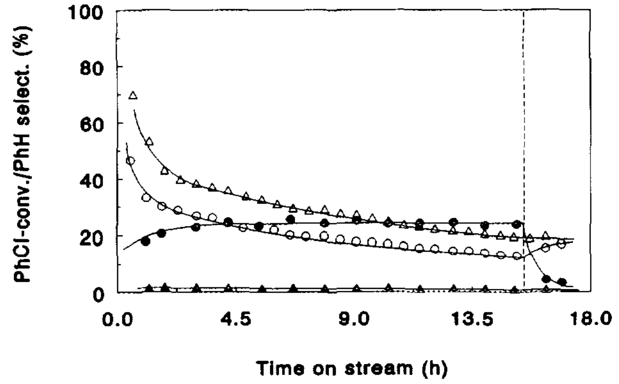

FIG. 8. Chlorobenzene conversion (○) and benzene selectivity (●) in the reaction with ammonia and hydrogen ($NH_3:H_2:PhCl$ ratio 20 : 10 : 1), vs time on stream. The dotted line shows the time at which the H_2 flow was switched off; data without additional H_2 [(△) and (▲), resp.] are shown for comparison. Catalyst, Cu-L-3.4; reaction temperature, 400°C.

catalytic activity of Cu/K-L-2.8 was tested for 16 h at 400°C; afterwards, thermo-gravimetric analysis was performed in air. Thus it was shown that the weight becomes constant after one hour at 450°C (see Fig. 7). For comparison, TGA data of Cu-silica-alumina are also shown.

The used Cu-L was treated in air (20 ml/min) for 16 h at 450°C; the material thus obtained was identical to the initial zeolite as shown by UV/vis, XRD, and IR measurements. Moreover, its catalytic properties were identical to the initial material, as shown in Table 3. Therefore, we conclude that Cu/K-L can be fully regenerated after application in the chlorobenzene amination. Identical results obtained with Cu/Na-mordenite indicate that all copper-exchanged zeolites can be regenerated in the procedure described.

4. *Mechanism of Benzene Formation*

Over several catalysts (Cu-Y, Cu-beta) major amounts of benzene were formed as a consequence of reductive dehalogenation. The results presented in Table 2 show that it is strongly affected by the type of zeolite used: in contrast to Cu-Y and Cu-beta, a limited dechlorination selectivity (≤3% at 400°C) is exhibited by Cu-L, Cu-ZSM-5, and Cu-mordenite. To investigate a possible role of hydrogen formed by ammonia decomposition, as proposed by Hatada *et al.* (6), we performed several experiments in which hydrogen was added to the feed; especially Cu-L was tested, because of its high activity. Figure 8 shows results obtained with a mixture of ammonia, hydrogen, and chlorobenzene (20 : 10 : 1), other conditions being identical to the previous experiments. An increase of the benzene selectivity was observed, along with a decrease of the overall conversion. Both effects are reversible, as all yields fall back to normal levels when the hydrogen flow is switched off.

XRD analysis of a catalyst after this reaction shows strong peaks at $2\theta = 43.3°–43.4°$ and 50.4°, caused by Cu^0 clusters (29). To investigate whether Cu^0 is involved in the formation of benzene, we pre-reduced a sample of Cu-L with hydrogen, followed by a reaction at 400°C with chlorobenzene as the only component (under conditions identical to those in the previous experiments). For comparison, an untreated Cu-L sample and a hydrogen-reduced ($CuCl_2$)K-L sample were also tested. The chlorobenzene conversions thus obtained are shown in Fig. 9,

TABLE 3

Use of Cu/K-L-2.8 in Two Consecutive Experiments, with an Air Treatment for 16 h at 450°C in between[a]

Time on stream (h)	Cu-L, fresh			Cu-L, regenerated		
	PhCl conv. (%)	$PhNH_2$ select. (%)	Ph_2NH select. (%)	PhCl conv. (%)	$PhNH_2$ select. (%)	Ph_2NH select. (%)
1	48	54	44	46	55	42
3	29	65	34	27	67	31
16	9	67	33	10	69	31

Note. Reaction temperature, 400°C; WHSV, 2.26 $h^{-1} \cdot (g_{total\ gas}/g_{cat})$; NH_3/PhCl ratio, 20 mol/mol.

[a] The selectivity balance is completed with formation of benzene.

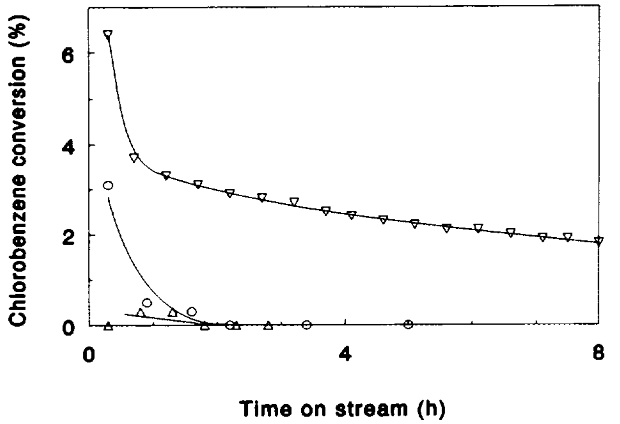

FIG. 9. Conversion of chlorobenzene to benzene, induced by several copper-containing zeolites: untreated Cu/K–L-2.8 (○), Cu^0/K–L (△), and Cu^0/H/K–L (▽). Reaction temperature, 400°C.

and XRD analysis, to obtain an impression of the amount of Cu^0 clusters, is shown in Fig. 10.

DISCUSSION

One of the advantages of zeolites as catalysts for organic reactions is the presence of metal ions as isolated catalytic sites. In our investigations, Cu(II)–zeolites are reduced to Cu^+/H^+ with ammonia (24, 28); during the chlorobenzene amination experiments, a continuous ammonia stream is supplied. Therefore, we conclude that the catalyst is mainly present as $Cu^+/(NH_4^+/H^+)$–zeolite. At lower temperatures, the metal ions are present as $Cu(NH_3)_2^+$ complexes (28); it is likely that the ammonia supplied during the reaction will maintain the catalytic active sites as $Cu(NH_3)_n^+$ ions.

The zeolites thus obtained show a remarkably high activity in the nucleophilic substitution when compared to copper-exchanged silica–alumina, because of the extremely high deactivation rate of the latter. The relatively low zeolite deactivation indicates that this phenomenon is related to the formation of heavier species, a process suppressed by the limited size of the zeolite channels. TGA analysis shows that a used Cu-silica–alumina contains at least 2 wt% nonvolatile products; this is lower than the amount observed on Cu–L after 16 h on stream (see Fig. 7), indicating that the larger condensation products which can be formed in the pores of silica–alumina have a more pronounced influence on the accessibility of the catalytic sites. The nonvolatile products formed on the zeolites can be formed on the outer zeolite surface, thereby contributing to the (lower) deactivation observed.

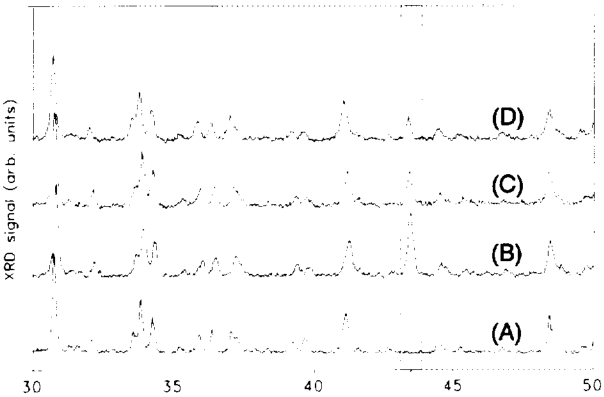

FIG. 10. XRD analysis of several copper-containing zeolites: untreated Cu/K–L-3.4 (A), Cu/K–L-3.4 after H_2/H_2O reduction (B), and sample (B) after reaction for 16 h with chlorobenzene (C) and chlorobenzene/ammonia (D) at 400°C.

When different zeolites are compared, large differences are observed in both activity and selectivity. The order of initial activities decreases according to Y ≈ L ≫ mordenite > beta > ZSM-5. This sequence runs roughly parallel to the increasing silica/alumina ratio. Different properties are likely to be responsible: the more polar surface of a low silica/alumina material should lead to a higher reactant concentration, especially of ammonia; alternatively, the actual substitution rate could be enhanced by the more polar environment, which acts as a "solid solvent." A combination of both effects is possible as well.

Comparing the catalytic activity (see Fig. 5) of Cu–L with the low-acidity $(CuCl_2)$K–L (*vide infra*), present as $(Cu^+Cl^-)K^+$–L, the results show clearly that the low-acidity sample gives a lower, but stable, chlorobenzene conversion. This indicates that the presence of acid sites is beneficial to the substitution reaction. Testing Cu–ZSM-5 in a similar reaction, the formation of phenol via a substitution of chlorobenzene with water, Perot *et al.* observed this effect as well (15): as in the experiments presented here, the presence of acidity increased the conversion. This was explained by a reaction mechanism in which acid sites play a role in the actual substitution. However, this phenomenon might also have another background. It is likely that the decomposition of a copper(I)-chloride complex, formed after the substitution, is an important step in the reaction mechanism; this decomposition might be enhanced by presence of acidity.

Comparing the selectivity patterns of the zeolites tested, a striking difference is the altering benzene formation. The results presented in Table 2 show an increasing benzene formation according to ZSM-5, mordenite, L < beta < Y. With increasing spaciousness of the pore system, the following phenomena are observed: the materials with smallest pore sizes, ZSM-5 (channel diameter about 5.5 Å) and mordenite (6.5 × 7 Å) show a low formation of benzene and diphenylamine, and therefore a high aniline selectivity (≥90%). The material with larger pores, zeolite L (7.1 Å), still shows a low formation of benzene, but a pronounced diphenylamine formation is observed. This indicates that shape selectivity is the determining factor in the low diphenylamine formation on mordenite and ZSM-5. However, the materials with even larger pores and intersections, beta (pores 6.4 × 7.6 Å, intersections about 11 Å) and especially Y (pores 7.4 Å, intersections about 13 Å) show a dramatic increase in benzene selectivity; besides, the diphenylamine selectivity decreases (down to <5% on Cu–Y), although there is no limitation caused by the zeolite channel size. Based on the observation that benzene formation seems related to decreased diphenylamine selectivity, with large-pore zeolites showing a high (Cu–Y) as well as a low (Cu–beta) chlorobenzene conversion, we conclude that the formation of benzene in the chlorobenzene amination is mainly caused by the decomposition of large condensation products.

This is in contrast to the observation of Hatada *et al.* (6), who concluded that hydrogen formed by the decomposition of ammonia might be responsible for the reduction towards benzene. Nitrogen formation from ammonia-adsorbed Cu–Y was also detected by Tanabe and Matsumoto (30), already at temperatures as low as 100°C. Indeed, we did observe that the presence of hydrogen resulted in a high formation of benzene (see Fig. 8). However, a hydrogen : chlorobenzene ratio of 10 : 1 only gave a benzene selectivity of about 25% on Cu–L. Besides, in additional experiments we showed that a mixture of chlorobenzene and aniline, in the absence of ammonia, also resulted in the formation of benzene (apart from diphenylamine, the normal substitution product) on both Cu–Y and Cu–L; therefore, it seems that the presence of ammonia is not required. Benzene formation caused by the decomposition of ammonia cannot be excluded, but the low benzene formation levels on zeolites Cu–L, Cu-mordenite, and Cu–ZSM-5 indicate that this process only plays a minor role.

As shown in Fig. 9, benzene is also formed from chlorobenzene without the addition of ammonia on a material pre-reduced to the Cu^0/H/K–L form. The data in Fig. 9 show that the presence of protons is required (as a hydrogen source for benzene formation), and that the Cu^0 clusters are consumed in the process (see Fig. 10). A similar effect, the reoxidation of Cu^0 in the presence of carbon monoxide (a compound which has, like ammonia, a high affinity to Cu^+) was observed by Sárkány *et al.* (31). Thus we presume that the following overall reaction scheme is responsible for the formation of benzene. Cu^0 is formed from copper ions present by reduction mainly with large condensation products: TGA analysis showed that Cu–L contained about 7 wt% nonvolatile condensation products after use for 16 h, as shown in Fig. 7. In this process, protons are formed as a charge compensation. Hereafter, the oxidation back to Cu^+ can take place during which chlorobenzene is converted to benzene. In the chlorobenzene–ammonia reaction, the XRD analysis did not reveal the presence of Cu^0 clusters; presumably the clusters are too small, and the reoxidation takes place rapidly. As shown in Fig. 8, the chlorobenzene conversion in the ammonia–hydrogen–chlorobenzene reaction decreases because the copper ions, the catalytically active sites, are reduced to Cu^0 by the hydrogen in the feed; however, after the hydrogen stream is switched off, the chlorobenzene conversion rapidly falls back to the normal level. This also supports a rapid reoxidation of Cu^0.

The results with Cu–mordenite, used for kinetic experiments, are shown in Fig. 6. The upper line shows the initial chlorobenzene conversions. For a simple first order reaction, a straight line should be obtained; the deviation can be explained by a higher sorption of reactants at lower temperatures, resulting in a higher surface concentration and therefore a higher conversion. Alternatively, depending on the temperature, the overall reaction order in chlorobenzene might be lower than the first order observed at 400°C (*vide infra*).

The lower line in Fig. 6, the conversion after prolonged (>16 h) time on stream, indicates that two regimes for deactivation exist in this reaction, resulting in a minimal deactivation around 400°C. The same phenomenon was also observed with Cu–L, showing that this minimal deactivation is not dependent on the type of zeolite. The deactivation at higher temperatures (400–450°C) can be explained by a higher formation of coke; it is likely that the low-temperature deactivation (350–400°C) is caused by a decreased desorption of products such as the side-product ammonium chloride (sublimation temperature 340°C) from the catalyst surface. Alternatively, diffusion limitation might also play a role at lower temperatures.

Based on our investigations, we propose the reaction scheme shown in Fig. 11. As to the actual substitution mechanism, preliminary results with chlorotoluene have shown that only *ipso*-substitution takes place, meaning that an arynic mechanism is not involved; this was also observed for the chlorobenzene substitution with water (15). On the other hand, a Michael-type ammonia addition would require high pressures of the nucleophile (13); therefore, this mechanism cannot take place either. There is, however, analogy with the Cu(I)-catalyzed homoge-

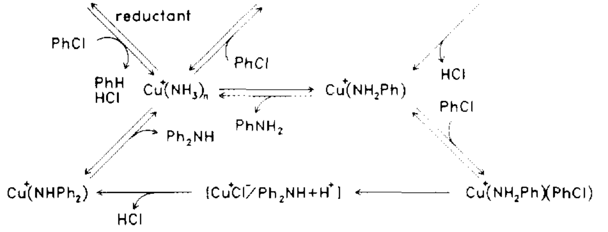

FIG. 11. Proposed reaction scheme for the conversion of chlorobenzene with ammonia. Ammonia adsorption and desorption have been omitted for clarity.

neous substitution of bromobenzene with sodium methoxide, in which $[Cu(CH_3O)_2]^-$ acts as a reaction intermediate (1). The $Cu(NH_3)_n^+$ complexes within the zeolite might interact likewise with chlorobenzene, either via the aromatic π system or via the halogen lone pairs. This indicates that the actual substitution can take place via single electron transfer (a Cu^+/Cu^{2+} couple) or coordinative interactions (2).

CONCLUSIONS

Copper-exchanged zeolites are active in the substitution of chlorobenzene with ammonia to form aniline; isolated copper(I) ions are assumed to be the active site, and acidity of the catalyst enhances the substitution rate. Especially Cu–mordenite and Cu–ZSM-5 are high selectivity catalysts: formation of both benzene and diphenylamine is limited because of shape-selectivity of the zeolites. The benzene formation on Cu–Y and Cu–beta is mainly caused by the decomposition of bulky condensation products; copper(0) clusters are assumed to be involved in this process.

The reaction has two deactivation regimes, depending on the temperature; these are a high-temperature region, in which coke formation occurs, and a low-temperature region, in which either the desorption of side-products is limiting or diffusion limitation takes place. At 400°C the deactivation is minimal.

ACKNOWLEDGMENTS

This work was financially supported by the Dutch Innovation Orientated Research Program on Catalysis. The authors thank Mr. O. Piekstra and Mr. B. Rölle for performing preliminary experiments, Mr. D. Demuth (University of Mainz, Germany) for the preparation of the Cu/Na–ZSM-5 sample, and Mr. M. S. Rigutto for many helpful discussions.

REFERENCES

1. Aalten, H. L., v. Koten, G., Grove, D. M., Kuilman, T., Piekstra, O. G., Hulshof, L. A., and Sheldon, R. A., *Tetrahedron* **45,** 5565 (1989).
2. Lindley, J., *Tetrahedron* **40,** 1433 (1984), and references therein.
3. Cf. Hölderich, W. F., and van Bekkum, H., *Stud. Surf. Sci. Catal.* **58,** 631 (1991).
4. Jones, D. G., U.S. Patent 3.231.616 (1966).
5. Venuto, P. B., and Landis, P. S., *Adv. Catal.* **18,** 259 (1968).
6. Hatada, K., Ono, Y., and Keii, T., *Adv. Chem. Ser.*, 501 (1973).
7. Warawdekar, M. G., and Rajadhyaksha, R. A., *Zeolites* **7,** 574 (1987).
8. Pitale, K. K., Warawdekar, M. G., and Rajadhyaksha, R. A., *in* "Adv. Catal. [Proc. 7th Natl. Symp. Catal.]," (T. S. R. Prasada Rao, Ed.), p. 263 Wiley, New York, 1985.
9. Chang, C. D., and Lang, W. H., U.S. Patent 4.380.699 (1983).
10. Palekar, M. G., *J. Catal.* **134,** 373 (1992).
11. Warawdekar, M. G., and Rajadhyaksha, R. A., *Zeolites* **7,** 579 (1987).
12. Chang, C. D., and Perkins, P. D., *Zeolites* **3,** 298 (1983).
13. Stamm, Th., Kouwenhoven, H. W., and Prins, R., *Stud. Surf. Sci. Catal.* **78,** 543 (1993).
14. Ishida, H., and Nakajima, H., Japanese Patents 62.240.634, 62.240.635, and 62.240.636 (1987).
15. Perot, G., Pouilloux, Y., Guisnet, M., and Gubelmann, M., *in* "Catalysis of Organic Reactions" (J. R. Kosak and T. A. Johnson, Eds.), p. 327 Marcel Dekker, New York, 1994.
16. Furuya, M., and Nakajima, H., Japanese Patent 03.206.060 (1991).
17. Cf. Iwamoto, M., *Stud. Surf. Sci. Catal.* **60,** 327 (1991).
18. Cf. Mizumoto, M., Yamazoe, N., and Seiyama, T., *J. Catal.* **55,** 119 (1978).
19. Sato, S., Yu-u, Y., Yahiro, H., Mizuno, N., and Iwamoto, M., *Appl. Catal.* **70,** L1 (1991), and references therein.
20. Kim, S. H., and Chon, H., *Appl. Catal. A* **85,** 47 (1992).
21. Oudejans, J. C., van der Gaag, F. J., and van Bekkum, H., *in* "Proc. 6th Int. Zeolite Conference" (D. Olson and A. Bisio, Eds.), p. 536 Butterworths, London, 1984.
22. Maxwell, I. E., Downing, R. S., and v. Langen, S. A. J., *J. Catal.* **61,** 485 (1980).
23. Maxwell, I. E., de Boer, J. J., and Downing, R. S., *J. Catal.* **61,** 493 (1980).
24. Maxwell, I. E., and Drent, E., *J. Catal.* **41,** 412 (1976).
25. Wortel, T. M., European Patent 96.479 (1983).
26. Wadlinger, R. L., Kerr, G. T., and Rosinski, E. J., U.S. Patent 3.308.069 (1967).
27. Piffer, R., Hagelstein, M., Cunis, S., Rabe, P., Förster, H., and Niemann, W., *Stud. Surf. Sci. Catal.* **69,** 259 (1991).
28. Huang, Y. Y., *J. Catal.* **30,** 187 (1973).
29. JCPDS—index 4-836, International Centre for Diffraction Data, Swarthmore (1988).
30. Tanabe, S., and Matsumoto, H., *Chem. Lett.*, 1425 (1985).
31. Sárkány, J., d'Itri, J. L., Sachtler, W. M. H., *Catal. Lett.* **16,** 241 (1992).